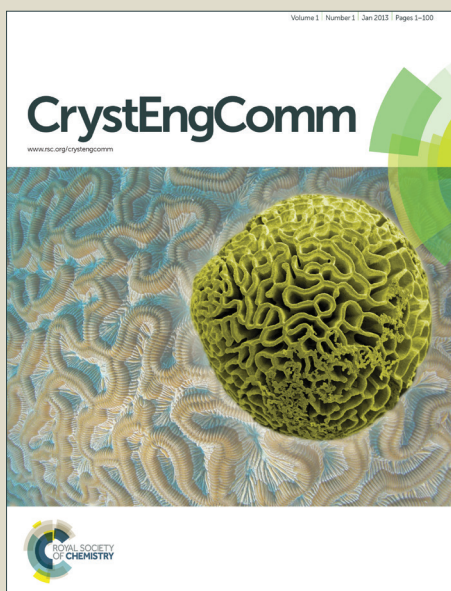


# CrystEngComm

Accepted Manuscript



This is an *Accepted Manuscript*, which has been through the Royal Society of Chemistry peer review process and has been accepted for publication.

*Accepted Manuscripts* are published online shortly after acceptance, before technical editing, formatting and proof reading. Using this free service, authors can make their results available to the community, in citable form, before we publish the edited article. We will replace this *Accepted Manuscript* with the edited and formatted *Advance Article* as soon as it is available.

You can find more information about *Accepted Manuscripts* in the [Information for Authors](#).

Please note that technical editing may introduce minor changes to the text and/or graphics, which may alter content. The journal's standard [Terms & Conditions](#) and the [Ethical guidelines](#) still apply. In no event shall the Royal Society of Chemistry be held responsible for any errors or omissions in this *Accepted Manuscript* or any consequences arising from the use of any information it contains.

## ARTICLE

## Green synthesis of nanorod Ni(salen) coordination complex by simple hydrothermal method

Cite this: DOI: 10.1039/x0xx00000x

M. Mohammadikish\*

Received 00th January 2012,  
Accepted 00th January 2012

DOI: 10.1039/x0xx00000x

[www.rsc.org/](http://www.rsc.org/)

One dimensional nanorods of Ni(salen) coordination compound were synthesized by facile hydrothermal route in green solvent at various times and temperatures without any surfactant or capping agent. The structure and morphology of the as-prepared complexes were investigated by using elemental analysis,  $^1\text{H}$  NMR, Fourier transform infrared spectroscopy (FT-IR), UV-Vis spectroscopy, X-ray diffraction (XRD), scanning electron microscopy (SEM), transmission electron microscopy (TEM) and thermogravimetric analysis (TGA).  $^1\text{H}$  NMR, FT-IR and elemental analysis confirmed the formation of Ni(salen) complex. The SEM and TEM images revealed that the products were nanorods with diameter of about 40-50 nm. Comparison of the Ni(salen) complexes prepared by hydro-/solvothetical method in different solvents ( $\text{H}_2\text{O}$ , EtOH and  $\text{CH}_3\text{CN}$ ), as well as Ni(salen) in reflux condition, illustrate that the product of hydrothermal route has more purity. The reasonable growth mechanism for the formation of Ni(salen) nanorods complex is also proposed.

**Keywords:** nanocomplex, nanorod, hydrothermal, Ni(salen)

### Introduction

One-dimensional (1D) nanostructured materials, such as nanorods, nanowires, nanotubes, nanobelts and nanoribbons, have attracted much attention in the emerging fields of nanoscience and nanotechnology because of their unique physical and chemical properties, and their promising applications in electronic and optoelectronic nanodevices [1–4]. Solvothermal synthesis is widely used as a mild and feasible method in the preparation of 1D inorganic nanomaterials [5].

Metal coordination compounds have been widely studied as they represent an important interface between material science and synthetic chemistry. Preparation of metal coordination compounds with different ligands and metal ions have led to a

wide range of potential applications as molecular magnets [6, 7], molecular wires [8–11], host-guest chemistry [12–15], electrical conductors [16–18], and catalysis [19]. The potential use of coordination complexes as materials for nanotechnological applications would seem to be very extensive as nanometer-scaled materials often exhibit new interesting size-dependent physical and chemical properties that cannot be observed in their bulk counterparts.

Over the past years, hydrothermal synthesis has rapidly developed as a new bridge between coordination chemistry and organic chemistry which represents a potential new direction for the construction of metal–organic frameworks through crystal engineering [20]. Under hydrothermal conditions, a variety of synthetic pathways have been tested and completed successfully including hydrolysis, oxidation, reduction and substitution reactions of ligands [21].

Synthesis of coordination compounds under hydro-/solvothetical conditions at relatively low temperatures of 100–200 °C has received much attention due to the ability of producing complexes with novel structures and properties. Additionally, Schiff base coordination complexes are still of great importance because of their simple preparation, diverse chemical structures, wide applications such as catalysis, biological modeling, material chemistry and molecular magnets [22–27]. However, reports on the hydrothermal syntheses of Schiff base coordination complexes are limited. Saghatforoush et al. synthesized Ni-Schiff base [28] and Cu-Schiff base [29] complexes by sonochemical and solvothermal methods. Liu et al. used N-p-nitrophenylsalicylaldiminewith zinc acetate and cadmium chloride respectively as precursors to synthesize Zn-

\* Faculty of Chemistry, Kharazmi University, Tehran, Iran  
Tel./fax: +98 26 34551023.  
E-mail address: mohammadikish@khu.ac.ir

Schiff base [30] and Cd-Schiff base [31] nanoribbons via solvothermal routes. Bis(8-hydroxyquinoline) magnesium [32] and bis(8-hydroxyquinoline) mercury [33] nanoribbons have been synthesized via solvothermal method by Wang et al.

Although Schiff base derived from ethylenediamine and salicylaldehyde (salen) can be readily prepared, to the best of our knowledge the hydro/solvothermal synthesis of their Schiff-base complexes has not been reported. In this study, uniform nanorods of Ni(salen) coordination compound were synthesized by a simple hydrothermal process. The synthesis was performed in aqueous solution without addition of any surfactant or capping agent. Characterization of the prepared material indicated that it consists of nanorods with the diameter of 30–40 nm. Furthermore, the possible formation mechanism was proposed which explains the crystal growth process well.

## Experimental

### Materials and methods

All reagents and solvents were of analytical grade and were used as received without further purification. The elemental analysis was carried out on a Perkin-Elmer 2400. The electronic spectra were recorded on Perkin-Elmer lambda 25 spectrometer. Fourier-transform infrared spectra were recorded using Perkin-Elmer Spectrum RXI FT-IR spectrometer, using pellets of the materials diluted with KBr.  $^1\text{H}$  NMR spectra were recorded on a Bruker Avance 300 spectrometer. The  $^1\text{H}$  NMR chemical shifts in ppm are reported from tetramethylsilane (TMS) as internal reference. X-ray diffraction patterns were recorded by a Rigaku D-max CIII, X-ray diffractometer using Ni-filtered Cu K $\alpha$  radiation. Scanning electron microscopy (SEM) images were obtained on KYKY-EM3200. Transmission electron microscopy (TEM) images were obtained on a Philips EM 208 instrument with an accelerating voltage of 100 kV. Thermogravimetric analysis (TGA) measurements were performed on a Perkin Elmer Diamond thermogravimeter in the temperature range from room temperature to 800 °C at a heating rate of 10 °C min $^{-1}$  in air.

### General procedure for the synthesis of Ni(salen)

#### Nano Ni(salen)

In a typical synthesis, 0.75 mmol of Ni(NO $_3$ ) $_2$ ·6H $_2$ O dissolved in 30 mL H $_2$ O was added to 0.75 mmol of N,N'-Bis(salicylidene)ethylenediamine dispersed in 70 mL H $_2$ O. The resulting mixture stirred for 15 min and then transferred into a teflon lined stainless steel autoclave with 150 mL capacity, sealed and maintained at various times and temperatures. After hydrothermal treatment, the autoclave cooled down to room temperature. The red-orange precipitate was collected and washed several times with distilled water and absolute ethanol. In some experiments, in solvothermal process 30 mL of C $_2$ H $_5$ OH or CH $_3$ CN were used as solvent instead of water.

#### Bulk Ni(salen)

For comparison, 0.75 mmol of N,N'-Bis(salicylidene)ethylenediamine and 0.75 mmol of Ni(NO $_3$ ) $_2$ ·6H $_2$ O were dissolved in 30 mL methanol and

refluxed for 2 hours. After evaporation of solvent fine crystals of bulk-Ni(salen) were appeared, that was filtered and washed with water and ethanol.

*1- Ni(salen). 0.3 H $_2$ O:* in reflux condition: red crystal (41%); Elemental anal. Calc. for C $_{16}$ H $_{14}$ N $_2$ O $_2$ Ni: C, 58.16; H, 4.45; N, 8.48. Found: C, 57.78; H, 4.06; N, 8.60.  $^1\text{H}$  NMR (DMSO- $d_6$ ):  $\delta$  = 7.89 (s, 2H, N=CH), 7.25 (dd, 2H, H $^{4,4'}$ ), 7.16 (dt, 2H, H $^{2,2'}$ ), 6.69 (d, 2H, H $^{1,1'}$ ), 6.50 (dt, 2H, H $^{3,3'}$ ), 3.41 (s, 4H, H $^{6,6'}$ ) ppm. FT-IR (KBr, cm $^{-1}$ ): 3420 ( $\nu_{\text{O-H}}$ , H $_2$ O), 3052, 3023 ( $\nu_{\text{C-H}}$ -aromatic), 2931 ( $\nu_{\text{C-H}}$ -aliphatic), 1623 ( $\nu_{\text{C=N}}$ ), 1600, 1536, 1451 ( $\nu_{\text{C=C}}$ ), 1127 ( $\nu_{\text{C-O}}$ ). UV-Vis ( $\lambda_{\text{max}}$ , nm, DMSO): 340, 408.

*2- Ni(salen). 0.1 H $_2$ O:* in 140°C-6h: red-orange (54%); Elemental anal. Calc. for C $_{16}$ H $_{14}$ N $_2$ O $_2$ Ni: C, 59.13; H, 4.34; N, 8.62. Found: C, 58.82; H, 4.24; N, 8.61.  $^1\text{H}$  NMR (DMSO- $d_6$ ):  $\delta$  = 7.89 (s, 2H, N=CH), 7.23 (dd, 2H, H $^{4,4'}$ ), 7.16 (dt, 2H, H $^{2,2'}$ ), 6.68 (d, 2H, H $^{1,1'}$ ), 6.50 (dt, 2H, H $^{3,3'}$ ), 3.41 (s, 4H, H $^{6,6'}$ ) ppm. FT-IR (KBr, cm $^{-1}$ ): 3426 ( $\nu_{\text{O-H}}$ , H $_2$ O), 3053, 3025 ( $\nu_{\text{C-H}}$ -aromatic), 2931 ( $\nu_{\text{C-H}}$ -aliphatic), 1624 ( $\nu_{\text{C=N}}$ ), 1600, 1536, 1451 ( $\nu_{\text{C=C}}$ ), 1128 ( $\nu_{\text{C-O}}$ ). UV-Vis ( $\lambda_{\text{max}}$ , nm, DMSO): 334, 404.

*3- Ni(salen). 0.1 H $_2$ O:* in 140°C-13h: red-orange (50%); Elemental anal. Calc. for C $_{16}$ H $_{14}$ N $_2$ O $_2$ Ni: C, 58.81; H, 4.38; N, 8.57. Found: C, 59.20; H, 4.00; N, 8.68.  $^1\text{H}$  NMR (DMSO- $d_6$ ):  $\delta$  = 7.89 (s, 2H, N=CH), 7.25 (d, 2H, H $^{4,4'}$ ), 7.16 (t, 2H, H $^{2,2'}$ ), 6.69 (d, 2H, H $^{1,1'}$ ), 6.50 (t, 2H, H $^{3,3'}$ ), 3.41 (s, 4H, H $^{6,6'}$ ) ppm. FT-IR (KBr, cm $^{-1}$ ): 3433 ( $\nu_{\text{O-H}}$ , H $_2$ O), 3052, 3024 ( $\nu_{\text{C-H}}$ -aromatic), 2930 ( $\nu_{\text{C-H}}$ -aliphatic), 1624 ( $\nu_{\text{C=N}}$ ), 1601, 1536, 1451 ( $\nu_{\text{C=C}}$ ), 1128 ( $\nu_{\text{C-O}}$ ). UV-Vis ( $\lambda_{\text{max}}$ , nm, DMSO): 320, 407.

*4- Ni(salen). 0.1 H $_2$ O:* in 140°C-18h: red-orange (46%); Elemental anal. Calc. for C $_{16}$ H $_{14}$ N $_2$ O $_2$ Ni: C, 59.13; H, 4.34; N, 8.62. Found: C, 59.16; H, 4.26; N, 8.67.  $^1\text{H}$  NMR (DMSO- $d_6$ ):  $\delta$  = 7.89 (s, 2H, N=CH), 7.25 (d, 2H, H $^{4,4'}$ ), 7.16 (t, 2H, H $^{2,2'}$ ), 6.69 (d, 2H, H $^{1,1'}$ ), 6.50 (t, 2H, H $^{3,3'}$ ), 3.41 (s, 4H, H $^{6,6'}$ ) ppm. FT-IR (KBr, cm $^{-1}$ ): 3433 ( $\nu_{\text{O-H}}$ , H $_2$ O), 3052, 3024 ( $\nu_{\text{C-H}}$ -aromatic), 2930 ( $\nu_{\text{C-H}}$ -aliphatic), 1624 ( $\nu_{\text{C=N}}$ ), 1599, 1536, 1451 ( $\nu_{\text{C=C}}$ ), 1127 ( $\nu_{\text{C-O}}$ ). UV-Vis ( $\lambda_{\text{max}}$ , nm, DMSO): 336, 409.

*5- Ni(salen). 0.2 H $_2$ O:* in 140°C-24h: red-orange (50%); Elemental anal. Calc. for C $_{16}$ H $_{14}$ N $_2$ O $_2$ Ni: C, 58.48; H, 4.42; N, 8.53. Found: C, 58.57; H, 4.25; N, 8.57.  $^1\text{H}$  NMR (DMSO- $d_6$ ):  $\delta$  = 7.89 (s, 2H, N=CH), 7.25 (d, 2H, H $^{4,4'}$ ), 7.16 (dt, 2H, H $^{2,2'}$ ), 6.69 (d, 2H, H $^{1,1'}$ ), 6.50 (t, 2H, H $^{3,3'}$ ), 3.41 (s, 4H, H $^{6,6'}$ ) ppm. FT-IR (KBr, cm $^{-1}$ ): 3435 ( $\nu_{\text{O-H}}$ , H $_2$ O), 3051, 3023 ( $\nu_{\text{C-H}}$ -aromatic), 2929 ( $\nu_{\text{C-H}}$ -aliphatic), 1623 ( $\nu_{\text{C=N}}$ ), 1600, 1536, 1451 ( $\nu_{\text{C=C}}$ ), 1128 ( $\nu_{\text{C-O}}$ ). UV-Vis ( $\lambda_{\text{max}}$ , nm, DMSO): 335, 409.

*6- Ni(salen). 0.1 H $_2$ O:* in 120°C-18h: red-orange (42%); Elemental anal. Calc. for C $_{16}$ H $_{14}$ N $_2$ O $_2$ Ni: C, 58.81; H, 4.38; N, 8.57. Found: C, 59.20; H, 4.10; N, 8.64.  $^1\text{H}$  NMR (DMSO- $d_6$ ):  $\delta$  = 7.89 (s, 2H, N=CH), 7.25 (dd, 2H, H $^{4,4'}$ ), 7.16 (dt, 2H, H $^{2,2'}$ ), 6.69 (d, 2H, H $^{1,1'}$ ), 6.50 (t, 2H, H $^{3,3'}$ ), 3.41 (s, 4H, H $^{6,6'}$ ) ppm. FT-IR (KBr, cm $^{-1}$ ): 3414 ( $\nu_{\text{O-H}}$ , H $_2$ O), 3052, 3024 ( $\nu_{\text{C-H}}$ -aromatic),

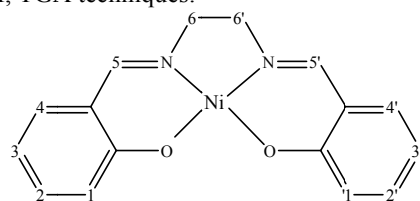
2930 ( $\nu_{\text{C-H-aliphatic}}$ ), 1624 ( $\nu_{\text{C=N}}$ ), 1600, 1536, 1451 ( $\nu_{\text{C=C}}$ ), 1128 ( $\nu_{\text{C-O}}$ ). UV-Vis ( $\lambda_{\text{max}}$ , nm, DMSO): 342, 408.

7- *Ni(salen)*. 0.2  $H_2O$ : in 160°C-18h: red-orange (50%); Elemental anal. Calc. for  $C_{16}H_{14}N_2O_2Ni$ : C, 58.48; H, 4.42; N, 8.53. Found: C, 58.42; H, 4.23; N, 8.53.  $^1H$  NMR (DMSO- $d_6$ ):  $\delta$  = 7.88 (s, 2H, N=CH), 7.24 (d, 2H,  $H^{4,4'}$ ), 7.16 (dt, 2H,  $H^{2,2'}$ ), 6.69 (d, 2H,  $H^{1,1'}$ ), 6.50 (t, 2H,  $H^{3,3'}$ ), 3.41 (s, 4H,  $H^{6,6'}$ ) ppm. FT-IR (KBr,  $cm^{-1}$ ): 3434 ( $\nu_{\text{O-H, H}_2\text{O}}$ ), 3052, 3022 ( $\nu_{\text{C-H-aromatic}}$ ), 2928 ( $\nu_{\text{C-H-aliphatic}}$ ), 1624 ( $\nu_{\text{C=N}}$ ), 1601, 1537, 1451 ( $\nu_{\text{C=C}}$ ), 1128 ( $\nu_{\text{C-O}}$ ). UV-Vis ( $\lambda_{\text{max}}$ , nm, DMSO): 330, 402.

8- *Ni(salen)*. 0.4  $H_2O$ : in 180°C-18h: red-orange (46%); Elemental anal. Calc. for  $C_{16}H_{14}N_2O_2Ni$ : C, 57.85; H, 4.49; N, 8.43. Found: C, 58.03; H, 4.13; N, 8.34.  $^1H$  NMR (DMSO- $d_6$ ):  $\delta$  = 7.88 (s, 2H, N=CH), 7.25 (d, 2H,  $H^{4,4'}$ ), 7.16 (t, 2H,  $H^{2,2'}$ ), 6.69 (d, 2H,  $H^{1,1'}$ ), 6.50 (t, 2H,  $H^{3,3'}$ ), 3.41 (s, 4H,  $H^{6,6'}$ ) ppm. FT-IR (KBr,  $cm^{-1}$ ): 3416 ( $\nu_{\text{O-H, H}_2\text{O}}$ ), 3052, 3024 ( $\nu_{\text{C-H-aromatic}}$ ), 2930 ( $\nu_{\text{C-H-aliphatic}}$ ), 1624 ( $\nu_{\text{C=N}}$ ), 1600, 1536, 1451 ( $\nu_{\text{C=C}}$ ), 1128 ( $\nu_{\text{C-O}}$ ). UV-Vis ( $\lambda_{\text{max}}$ , nm, DMSO): 330, 402.

## Results and discussion

The solid *Ni(salen)* complexes were synthesized with hydro-/solvothoermal treatment of *salen* ligand with nickel nitrate in molar ratio 1:1 at different temperatures (120 °C, 140 °C, 160 °C and 180 °C), times (6h, 13h, 18h and 24h) and solvents ( $H_2O$ ,  $C_2H_5OH$  and  $CH_3CN$ ). Structural and morphological characterization of the complexes was carried out by elemental analysis,  $^1H$  NMR, FT-IR, UV-Vis spectroscopies, and XRD, SEM, TEM, TGA techniques.



Scheme 1

The elemental analysis results of the hydrothermal products are in very good agreement with bulk complex that was synthesized in reflux conditions; although the CHN results of solvothoermal reactions e.g. 140 °C-6h in ethanol and 140 °C-6h in acetonitrile are somewhat different from calculated data.

The structure of the *Ni(salen)* complex is presented in Scheme 1. The  $^1H$  NMR spectra of the bulk sample and all of the nano complexes prepared in aqueous solution in different temperatures and times are quite similar. For all of them, the coordination of two phenolic oxygens to nickel center were confirmed by the absence of 10–12 ppm signal, typical of phenolic OH groups in ligand. The presence of one sharp singlet for the two azomethine protons in 7.89 ppm clearly suggested their equivalent environment in complex. The aromatic proton signals were appeared in the 7.25, 7.16, 6.69 and 6.50 ppm for  $H^{4,4'}$ ,  $H^{2,2'}$ ,  $H^{1,1'}$  and  $H^{3,3'}$  respectively. Also the observed sharp singlet in 3.41 ppm can be assigned to the four aliphatic hydrogens ( $H^{6,6'}$ ). For comparison, the  $^1H$  NMR spectra of samples 1 and 2 were shown in Fig. 1. For two solvothoermal

samples (140 °C-6h in ethanol and 140 °C-6h in acetonitrile) all of these signals exist as well as some impurities.

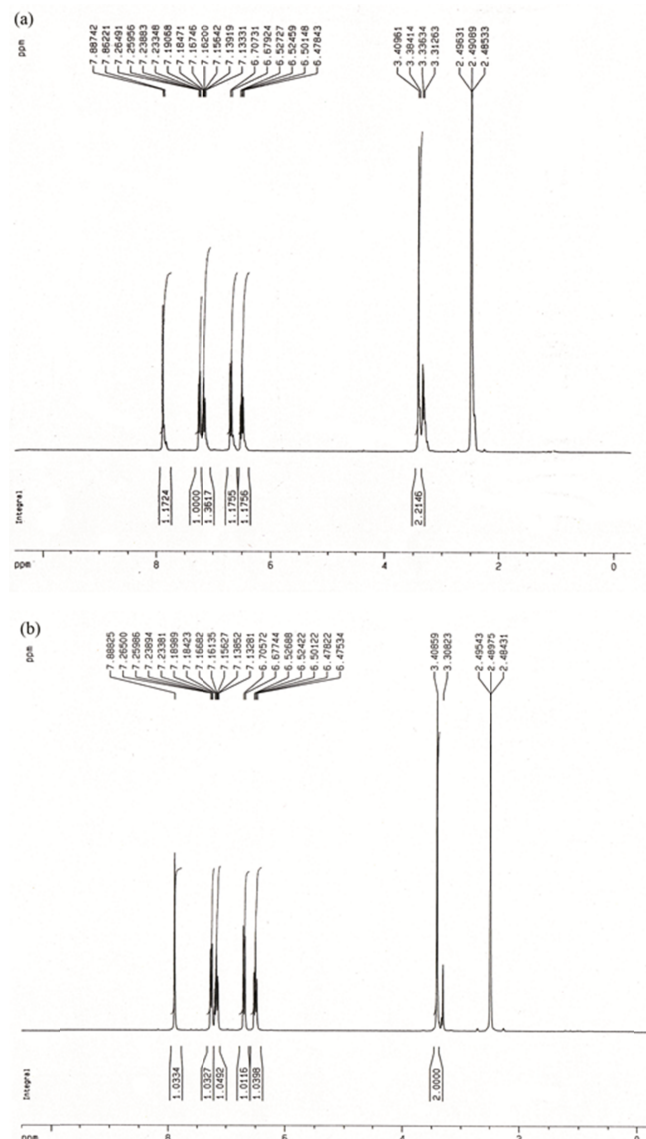
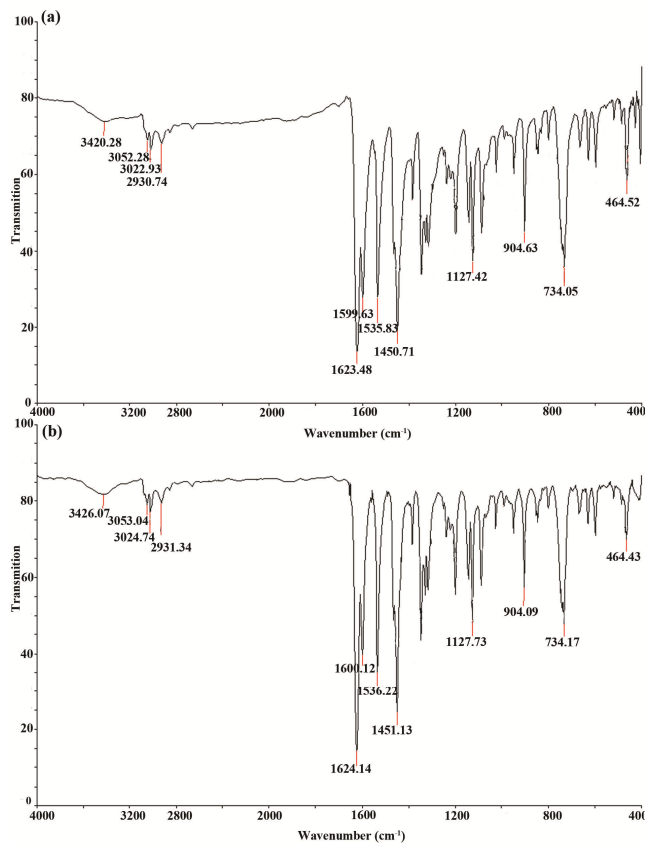


Fig. 1.  $^1H$  NMR spectra of *Ni(salen)* prepared at (a) reflux, and (b) hydrothermal conditions 140 °C-6h.

The FT-IR spectra of all complexes exhibited a broad band around 3400  $cm^{-1}$  which is attributed to the lattice or coordinating water molecules [34]. The spectra exhibited some weak bands at 2800–3100  $cm^{-1}$  that are related to aromatic and aliphatic C–H stretching vibrations. The strong band at 1624  $cm^{-1}$  can be assigned to the stretching vibrations of the azomethine groups which shifted to lower frequencies in the complexes due to the coordination of nitrogens to the nickel ion. The ring skeletal vibrations ( $\nu_{\text{C=C}}$ ) of the complex can be observed in the region of 1450–1600  $cm^{-1}$ . The band appeared at 1128  $cm^{-1}$  can be assigned to the phenolic C–O stretching vibrations that undergo a shift toward higher wave numbers with respect to the ligand [35]. Consequently, the FT-IR spectra showed good evidences for the synthesis of the solid complexes. The FT-IR spectra of samples 1 and 2 can be seen in Fig. 2.



**Fig. 2.** FT-IR spectra of Ni(salen) prepared at (a) reflux, and (b) hydrothermal conditions 140 °C-6h.

The electronic spectra of the Ni(II) complexes were similar and revealed two broad peaks around 335 and 405 nm. The first one can be assigned to the  $\pi$ - $\pi^*$  transition in the ligand and the next band may be attributed to the d-d transition for nickel complexes.

Fig. 3 shows XRD patterns of typical Ni(salen) complexes prepared by the hydrothermal process and indicates the crystalline nature of the products. The investigation of XRD patterns shows that the experimental data are in good agreement with the simulated XRD patterns obtained from single crystal data [36] which shows the phase purity of these compounds. All of the diffraction peaks were indexed by comparison with the simulated XRD powder patterns [36]. The higher intensity of (2 0 0) peak in 180 °C-18h revealed the preferred growth at the {1 0 0} orientation with addition of the time and temperature of the reaction.

The SEM images of Ni(salen) complexes are shown in Figures 4-7. The SEM image of the complex synthesized in reflux condition (Figure 4) indicated bulk sample without characteristic morphology.

The time-dependent morphology evolution study was conducted at 140 °C. Figure 4 indicates SEM images of hydrothermal preparation at 140 °C and various times. These images clearly reveal that the as-synthesized products are nanorods with thickness of about 30-40 nm.

The product obtained after 6h is consisted of separated nanorods (Fig. 5a,b). Extending the reaction time to 13h led to agglomeration of the product and formation of some nanoparticles (Fig. 5c,d). A mixture of nanorods and nanoparticles were formed after 18 h (Fig. 5e,f). After 24 h, the

more agglomerated nanorods with smaller length were seen (Fig. 5g,h).

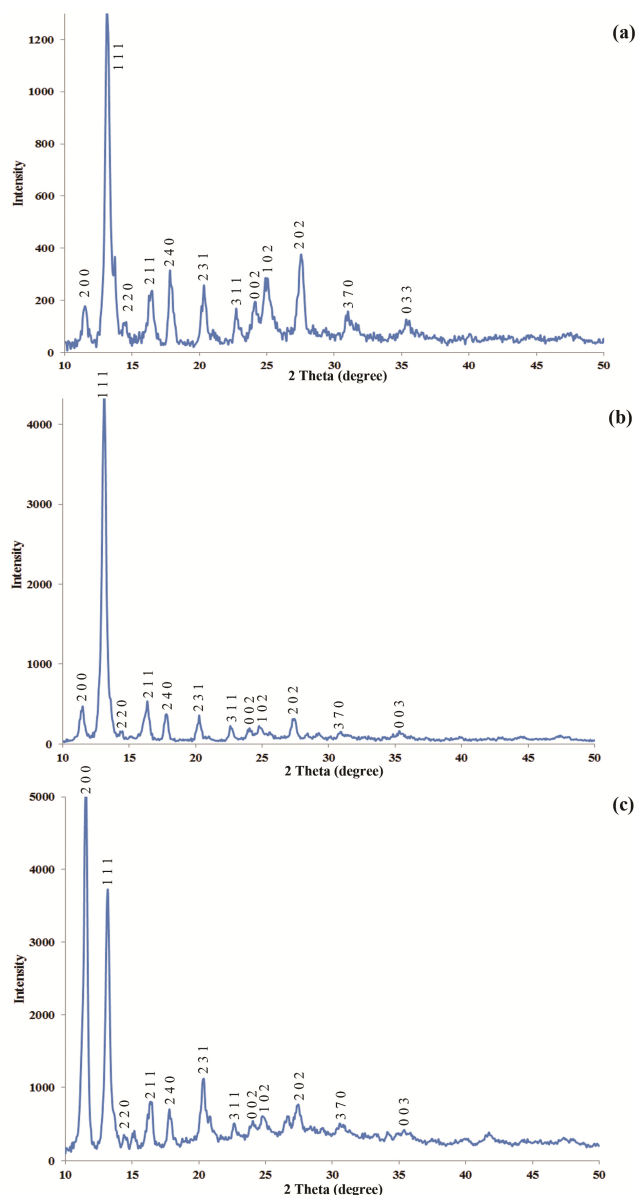


**Fig. 3.** XRD patterns of the as-prepared Ni(salen) at (a) 140 °C-6h (b) 140 °C-18h and (c) 180 °C-18h.

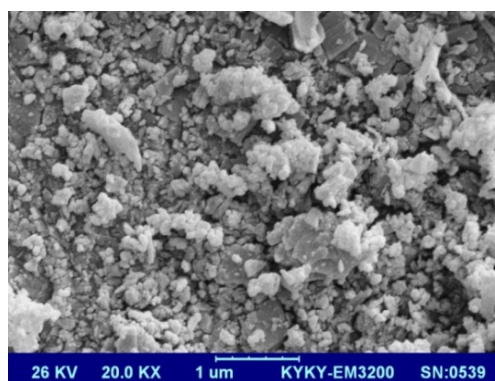


**Fig. 4.** SEM images of bulk Ni(salen) sample prepared in reflux condition.

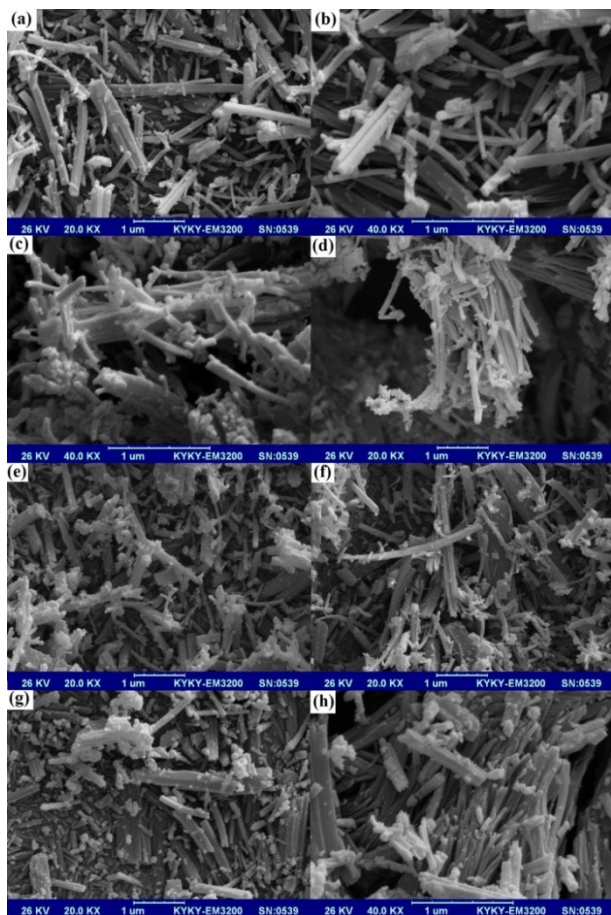


Fig. 5. SEM images of Ni(salen) nano complexes prepared in H<sub>2</sub>O at 140 °C and various times; (a,b) 6h, (c,d) 13h, (e,f) 18h, (g,h) 24h.

In addition to the reaction time, the effect of reaction temperature on the formation of the products was also studied at 18 h. At 120 °C, a mixture of nanorods and nanoplates (with thickness of 23 nm) were formed (Fig. 6a,b). When the temperature was raised to 140 °C, nanorods and in less extent nanoplates were produced (Fig. 6c,d). At 160 °C broken nanorods and nanoparticles were seen (Fig. 6e,f). Some agglomerated nanorods and nanoparticles were obtained at 180 °C (Fig. 6g,h). Therefore, it clearly shows that changing temperature and time can affect the morphology of the obtained nano complexes.

In addition to the reaction time and temperature, to investigate the effect of solvent, some solvothermal reactions were also carried out at 140 °C and 6h in H<sub>2</sub>O, C<sub>2</sub>H<sub>5</sub>OH and CH<sub>3</sub>CN as solvent. In hydrothermal route, in the presence of H<sub>2</sub>O separated nanorods were formed (Fig. 7a,b). In ethanol just nanoparticles with average size of 47 nm were produced (Fig. 7c,d) whereas in acetonitrile some nanorods with small length as well as nanoparticles were obtained (Fig. 7e,f).

The TEM image (Fig. 8) of Ni(salen) nano complex at 140 °C-6h clearly reveal that the as-prepared nanorods agglomerated to form bundles with small thickness.

The thermogravimetric (TG/DTG/DTA) curves of Ni(salen) nano complex at 140 °C-6h are presented in Fig. 9. From thermogravimetric investigation it is possible to observe that the thermal decomposition occurs in three steps. The complex is hydrated and lost water in the first weight loss and afterwards

the organic ligand residue is burned in two steps to left the metallic nickel in the final step. The complex completed the decomposition about 500 °C.

From the DTA curve it is obvious that the loss of water is endothermic. An intense exothermic decomposition peak was observed for organic residue burning about 460 °C.

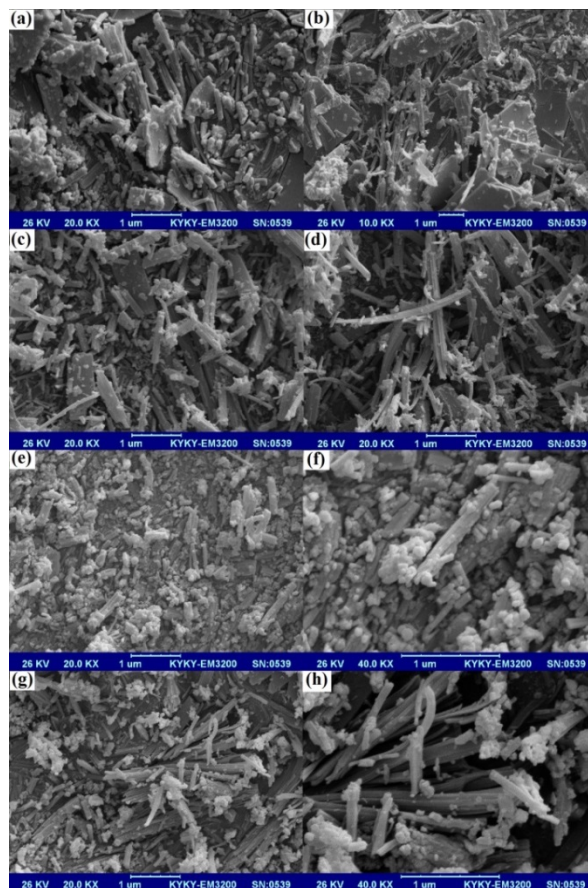


Fig. 6. SEM images of Ni(salen) nano complexes prepared in H<sub>2</sub>O at 18h and various temperatures; (a,b) 120 °C, (c,d) 140 °C, (e,f) 160 °C, (g,h) 180 °C.

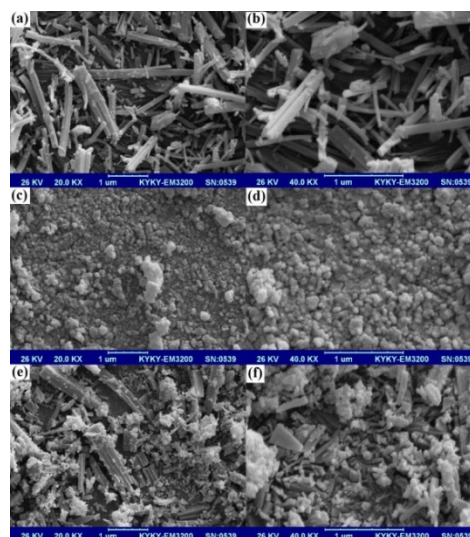


Fig. 7. SEM images of Ni(salen) nano complexes prepared at 140 °C-6h and various solvents; (a,b) H<sub>2</sub>O, (c,d) EtOH, (e,f) CH<sub>3</sub>CN.

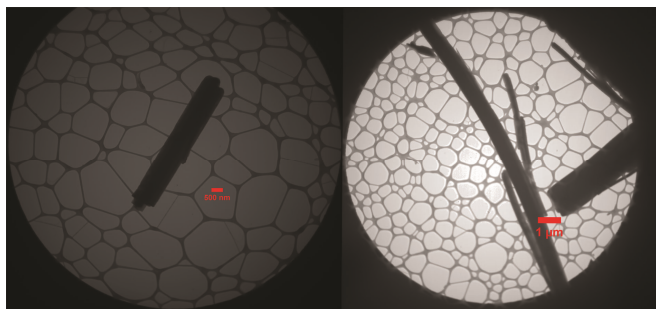


Fig. 8. TEM image of Ni(salen) nano complexes prepared at 140 °C-6h in H<sub>2</sub>O.

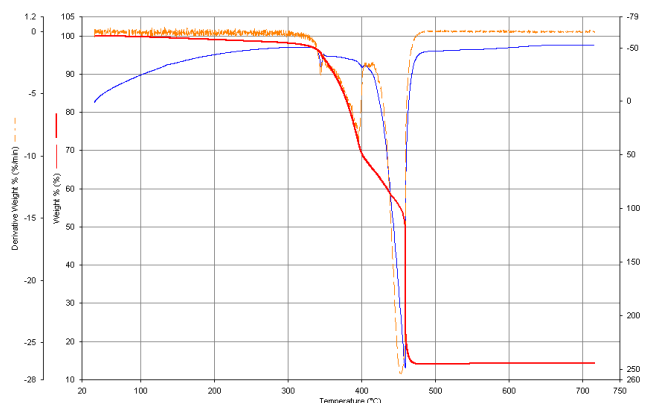
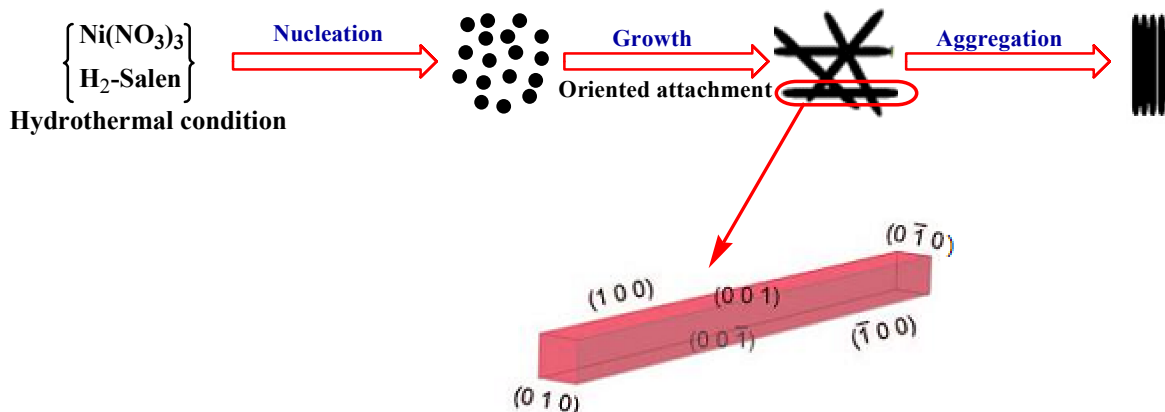


Fig.9. TGA, DTG and DTA curves of Ni(salen) nano complexes prepared at 140 °C-6h in H<sub>2</sub>O.



Scheme 2. Schematic illustration of a proposed mechanism for the formation of the Ni(salen) nanorods.

Based on the morphology evolution, the possible formation mechanism of nanorods Ni(salen) complex has been proposed as a sequential two-step growth mechanism, heterogeneous complex nucleation and directional growth route (Scheme 2). In the hydrothermal condition, the soluble Ni<sup>2+</sup> cation reacted with salen ligand to form insoluble Ni(salen) nucleus. This hydrothermal reaction can be ascribed to the precipitation transformation process in H<sub>2</sub>O, which the formation of more insoluble Ni(salen) was the driving force for this reaction. During the early stage, the Ni(salen) nucleates heterogeneously due to the fact that the energy barrier for this heterogeneous nucleation is lower than that for the nucleation in solution [37]. In the initial stage, large quantities of small primary nanocrystals were formed by nucleation under the hydrothermal condition. Because these small primary nanoparticles were unstable due to their high surface energy, they tend to aggregate rapidly and grow to rod-like nanostructures, probably driven by the oriented aggregation [38,39]. Then the nanorod gradually assembled to nanorod array through oriented attachment, in order to reduce the surface free energies to reach the thermodynamically stable structures.

According to the reported crystal structures [36, 40], Ni(salen) has tetragonal crystal lattice with {100}, {010} and {001} faces. The nanorods of Ni(salen) complex is the result of the faster growth rate along <010> direction. In all reported crystal structures, the <100> and/or <010> directions are the favored directions for crystal growth. Under the hydrothermal condition, the nuclei start to assemble together and spontaneously aggregate into nanorods to

minimize their surface area through the process known as oriented attachment [41]. As the reaction time prolonged, the Ostwald ripening process dominated, then the nanorods with smooth surface were generated.

Furthermore, the hydrothermal reaction time and temperature also affect the quality of the nanorods. If reaction time is less than 6 h at 140 °C, the uniform and regular Ni(salen) nanorods obtained. When reaction time or temperature was increased, the prepared Ni(salen) nanorods are broken and short nanorods or nanoparticle can be seen.

## Conclusions

In summary, Ni(salen) nanorods were successfully prepared in a one-step process by a simple hydrothermal route. SEM and TEM analysis showed that the nanorod size is controllable, with thickness about 30-40 nm. It has been found that the variations in reaction temperature and times have no significant effect on the shape and morphology of nano complexes but the change in solvent is effective. The morphology of Ni(salen) nanorods can be controlled by the faster growth rate along <010> direction.

## Acknowledgements

The author is grateful to Kharazmi University for financial support.

## References

- [1] J.T. Hu, T.W. Odom, C.M. Lieber, *Acc. Chem. Res.*, 1999, **32**, 435.

- [2] Z.W. Pan, Z.R. Dai, Z.L. Wang, *Science*, 2001, **291**, 1947.
- [3] M.W. Shao, Y.Y. Shan, N.B. Wong, S.T. Lee, *Adv. Funct. Mater.*, 2005, **15**, 1478.
- [4] G.Z. Shen, D. Chen, P.C. Chen, C.W. Zhou, *ACS Nano*, 2009, **3**, 1115.
- [5] F.X. Wang, M.W. Shao, L. Cheng, J. Hua, X.W. Wei, *Mater. Res. Bull.* 2009, **44**, 1687.
- [6] M.A.M. Abu-Youssef, A. Escuer, D. Gatteschi, M.A.S. Goher, F.A. Mautner, R. Vicente, *Inorg. Chem.* 1999, **38**, 5716.
- [7] A. Caneschi, D. Gatteschi, N. Lalioti, C. Sangregorio, *Angew. Chem. Int. Ed. Engl.* 2001, **40**, 1760.
- [8] K.-T. Wong, J.-M. Lehn, S.-M. Peng, G.-H. Lee, *Chem. Commun.* 2000, **22**, 2259.
- [9] J.A. Ramsden, W. Weng, A.M. Arif, J.A. Gladysz, *J. Am. Chem. Soc.* 1992, **114**, 5890.
- [10] W. Weng, J.A. Ramsden, A.M. Arif, *J. Am. Chem. Soc.* 1993, **115**, 3824.
- [11] N. Le Narvor, L. Toupet, C. Lapinte, *J. Am. Chem. Soc.* 1995, **117**, 7129.
- [12] M. Aoyagi, K. Biradha, M. Fujita, *J. Am. Chem. Soc.* 1999, **121**, 7457.
- [13] A. Tanatani, M.J. Moi, J.S. Moore, *J. Am. Chem. Soc.* 2001, **123**, 1792.
- [14] K. Biradh, C. Seward, M.J. Zaworotko, *Angew. Chem.* 1999, **111**, 584.
- [15] K. Biradh, C. Seward, M.J. Zaworotko, *Angew. Chem. Int. Ed. Engl.* 1999, **38**, 492.
- [16] J.S. Miller (Ed.), *Extended Linear Chain Compounds*, vol.1, Plenum Press, New York, 1982.
- [17] A. Aumuller, P. Erk, G. Klebe, S. Hunig, J.U. Von Schutz, H.-P. Werner, *Angew. Chem. Int. Ed. Engl.* 1986, **98**, 759.
- [18] A.G. Bunn, P.J. Carroll, B.B. Wayland, *Inorg. Chem.* 1992, **31**, 1297.
- [19] M. Fujita, Y.J. Kown, S. Washizu, K.J. Ogura, *J. Am. Chem. Soc.* 1994, **116**, 1151.
- [20] X.M. Chen, M.L. Tong, *Acc. Chem. Res.* 2006, **40**, 162.
- [21] J.Y. Lu, V. Schauss, *Eur. J. Inorg. Chem.* 2002, 1945.
- [22] S. Kotha, *Acc. Chem. Res.* 2003, **36**, 342.
- [23] M.J. O'Donnell, *Acc. Chem. Res.* 2004, **37**, 506.
- [24] H.C. Wu, P. Thanasekaran, C.H. Tsai, J.Y. Wu, S.M. Huang, Y.S. Wen, K.L. Lu, *Inorg. Chem.* 2006, **45**, 295.
- [25] M. Zhao, C. Zhong, C. Stern, A.G.M. Barrett, B.M. Hoffman, *J. Am. Chem. Soc.* 2005, **127**, 9769.
- [26] J.L. Sessler, E. Tomat, V.M. Lynch, *J. Am. Chem. Soc.* 2006, **128**, 4184.
- [27] S. Das, A. Nag, D. Goswami, P.K. Bharadwaj, *J. Am. Chem. Soc.* 2006, **128**, 402.
- [28] L.A. Saghatforoush, R. Mehdizadeh, F. Chalabian, *Transition Met. Chem.* 2010, **35**, 903.
- [29] L.A. Saghatforoush, R. Mehdizadeh, F. Chalabian, *J. Chem. Pharm. Res.* 2011, **3**, 691.
- [30] L. Liu, M.W. Shao, X.H. Wang, *J. Solid State Chem* 2010, **183**, 590.
- [31] L. Liu, Z. Zhang, *Front. Optoelectron. China*, 2011, **4**, 199.
- [32] X. Wang, M. Shao, L. Liu, *Thin Solid Films*, 2010, **519**, 231.
- [33] L. Liu, M. Shao, X. Wang, *Front. Optoelectron. China*, 2011, **3**, 228.
- [34] A.B.P. Lever, *Inorganic Electronic Spectroscopy*, second ed., Elsevier, New York, 1984.
- [35] W.H. Correa, S. Papadopoulos, P. Radnidge, B.A. Roberts, J.L. Scott, *Green Chem.* 2002, **4**, 245.
- [36] A.G. Manfredoti, C. Guastini, *Acta Cryst. C*, 1983, **39**, 863.
- [37] L.J. Luo, W. Tao, X.Y. Hu, T. Xiao, B.J. Heng, W. Huang, H. Wang, H.W. Han, Q.K. Jiang, J.B. Wang, Y.W. Tan, *J. Power Sources*, 2011, **196**, 10518.
- [38] X.L. Hu, J.C. Yu, *Adv. Funct. Mater.* 2008, **18**, 880.
- [39] L.P. Zhu, H.M. Xiao, S.Y. Fu, *Cryst. Growth Des.* 2007, **7**, 177.
- [40] M.A. Siegler, M. Lutz, *Cryst. Growth Des.* 2009, **9**, NO. 1194.
- [41] Q. Zhang, S.J. Liu, S.H. Yu, *J. Mater. Chem.* 2009, **19**, 191.